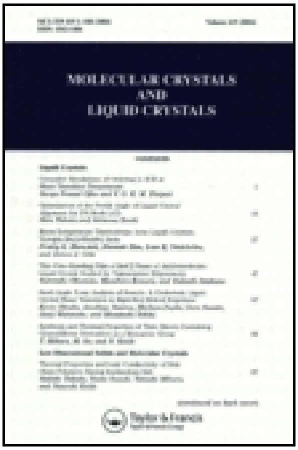

Molecular Crystals and Liquid Crystals
Publication details, including instructions for authors and subscription information:
http://www.tandfonline.com/loi/gmcl18

Structural Changes Occurring in the Phase Transition of Ferroelectric Liquid Crystals [I Temperature Dependence of the X-Ray Diffraction and FTIR/Raman Spectra

Kohji Tashiro [a] , Jian-An Hou [a] & Masamichi Kobayashi [a]

[a] Department of Macromolecular Science, Faculty of Science, Osaka University, Toyonaka, Osaka, 560, Japan

Version of record first published: 04 Oct 2006.

To cite this article: Kohji Tashiro , Jian-An Hou & Masamichi Kobayashi (1991): Structural Changes Occurring in the Phase Transition of Ferroelectric Liquid Crystals [I Temperature Dependence of the X-Ray Diffraction and FTIR/Raman Spectra, Molecular Crystals and Liquid Crystals, 200:1, 145-155

To link to this article: http://dx.doi.org/10.1080/00268949108044237

Mol. Cryst. Liq. Cryst., 1991, Vol. 200, pp. 145–155
Reprints available directly from the publisher
Photocopying permitted by license only

Printed in the United States of America

Structural Changes Occurring in the Phase Transition of Ferroelectric Liquid Crystals [I] Temperature Dependence of the X-Ray Diffraction and FTIR/Raman Spectra

KOHJI TASHIRO, JIAN-AN HOU and MASAMICHI KOBAYASHI

Department of Macromolecular Science, Faculty of Science, Osaka University, Toyonaka, Osaka 560, Japan

(Received September 4, 1990; in final form December 14, 1990)

Structural changes in the ferroelectric liquid crystal of chiral 4-*n*-hexyloxyphenyl 4′-[2-methylheptyloxy]-biphenyl-4-carboxylate,

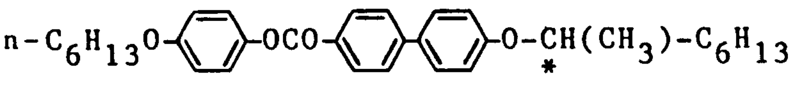

were analyzed by means of X-ray diffraction, FTIR, Raman and DSC measurements. Many different types of crystal modifications were found to be generated depending on the crystallization conditions such as the cooling rate from the isotropic phase, the type of solvents, etc. These crystal phases experience crystal-to-crystal and crystal-to-liquid crystal phase transitions, in which the interlamellar spacing and the packing fashion of the molecules change drastically, as revealed by the X-ray diffraction data. The Raman and FTIR spectral measurements clarified that the molecular conformations were thermally agitated during the phase transitions: the alkyl chains are disordered and the biphenyl groups are twisted in the liquid-crystalline and isotropic phases. In the ferroelectric phase transition between the chiral smectic C and cholesteric phases, the electric dipoles locating around the

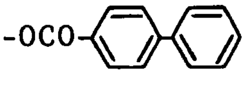

part are considered to change their orientation directions through the internal rotation of the biphenyl groups, resulting in the change in bulk electric polarization.

Keywords: ferroelectric liquid crystal, phase transition, structure, X-ray diffraction, infrared spectra, Raman spectra

INTRODUCTION

A great deal of attention has been paid to ferroelectric liquid crystals (FLC) because of their excellent electrical properties,[1–8] compared with those of conventional liquid crystals. The characteristic behavior is manifested particularly in the chiral smectic C (S_c^*) phase. The macroscopic structural parameters such as the helical pitch, the tilt angle of the molecular axis from the normal of layer, etc. have been found to change drastically in the S_c^* to S_A^* (or S_c^* to cholesteric) phase transition.[9–13] However, only little has been known about the molecular level structures of liquid-crystalline phases. This is because of difficulty in structural analysis by X-ray diffraction, i.e., liquid-crystalline phases give very poor diffraction data. One useful approach is to investigate the changes in X-ray diffraction as well as IR and Raman spectra on the phase transition from crystal (C) to liquid crystal (LC) and infer the structure of LC based on that of C. The use of spectroscopic method is powerful in this approach, because it provides the information about each part of such complicated molecule as FLC, regardless of the aggregation state. Thus we started the study on the phase transition of a FLC material with the following chemical structure.

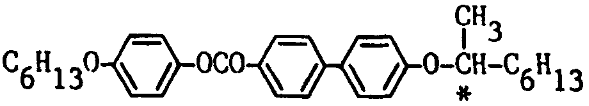

However, we found that this compound appeared in various modifications depending on the crystallization condition and thermal history. Therefore, it became

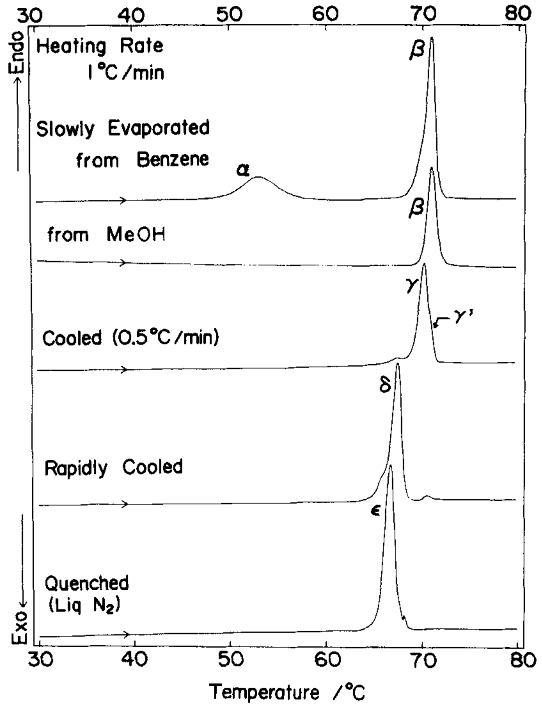

FIGURE 1 DSC thermograms of the samples prepared under various conditions.

necessary to clarify first the complicated feature of crystalline polymorphs and the phase transition behavior among them on a heating process toward the S_c^* phase.

The present work deals with crystal modifications which appear in different crystallization conditions and phase transitions on a heating process starting from one of the crystal forms (names α which is stable in low-temperature range) toward the S_c^* phase, investigated by X-ray diffraction, vibrational spectroscopy, and thermal analysis.

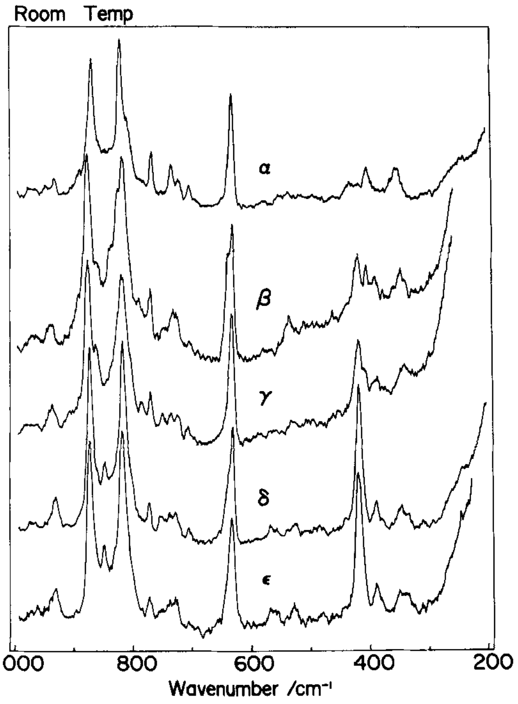

FIGURE 2 Raman spectra of the crystal forms α–ε taken at room temperature.

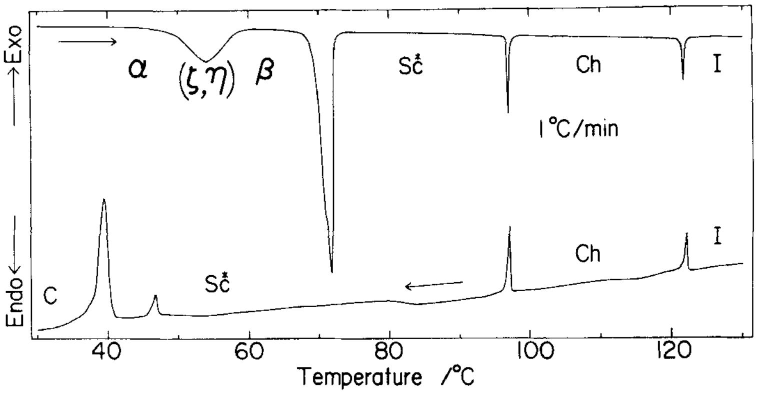

FIGURE 3 DSC thermogram of the α form.

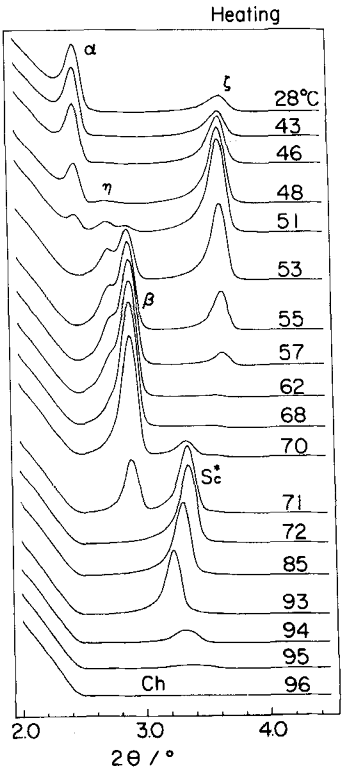

FIGURE 4 A change of the X-ray diffraction pattern in the heating process from the α crystal form. The sample contains some amount of the ζ form even at the initial stage.

EXPERIMENTAL SECTION

Thermal behavior of the above-mentioned FLC was analyzed by a SEIKO-DSC20 Differential Scanning Calorimeter with heating and cooling rates of 0.1–2.0°C/min. The X-ray powder patterns were obtained by a Rigaku RAD-ROC diffractometer with a graphite-monochromatized Cu-K_α radiation (λ = 1.5418 Å). The temperature dependence of the X-ray diffraction pattern was measured on the sample set into a home-made furnace (temperature fluctuation within ±0.5°C). The temperature dependence of the infrared absorption spectra was measured with a Japan Spectroscopic Co. (JASCO) Fourier-Transform Infrared Spectrometer (FT/IR-8000) on powdered samples in a KBr disk. The Raman spectra were measured with a JASCO R-500 Spectrometer. The 514.5 nm line from an Ar^+ gas laser was used as an excitation light source. The powder sample was packed into a glass capillary. The temperature dependence of the Raman spectra was measured using a hand-made heater made of copper block controlled with a temperature fluctuation less than ±0.5°C.

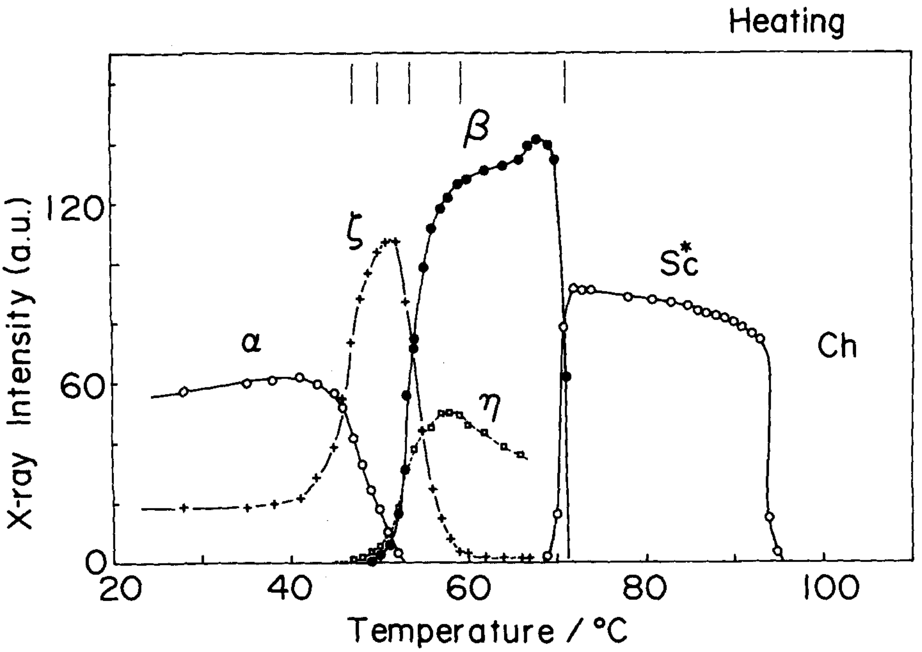

FIGURE 5 Temperature dependence of the X-ray peak intensity (heating process). The initial sample is a mixture of the α and ζ forms.

RESULTS AND DISCUSSION

Crystal Modifications

The present FLC compound exhibits a variety of crystal (and/or liquid crystal) modifications depending on the crystallization conditions such as the cooling rate from the neat isotropic phase, the evaporation rate of the solvent from solution, and so on. As shown in Figure 1, for example, the α form is obtained by slow solvent evaporation from a benzene solution. The β form crystallized from a methanol solution can be also obtained by a slow cooling of the isotropic phase. The other modifications of γ, γ′, δ etc. are prepared by relatively rapid cooling or quenching from the isotropic state down to liquid nitrogen temperature. The α form transfers into the β form and then into the S_c^* phase. The other phases transform into the S_c^* at temperatures different from each other. Thus, it should be emphasized here that this FLC compound exhibits quite complicated crystallization and thermal behavior affected sensitively by a slight change in the sample preparation condition. Thermal behavior of liquid crystals is often measured by the DSC method as a convenient technique. But, as seen in the present case, careful attention should be paid to the heating and/or cooling rates in the DSC measurement.

In Figure 2 the Raman spectra taken for these crystal modifications at room temperature are compared. The Raman bands associated with the benzene, biphenyl, ester, and alkyl groups are observed with different relative intensities. In

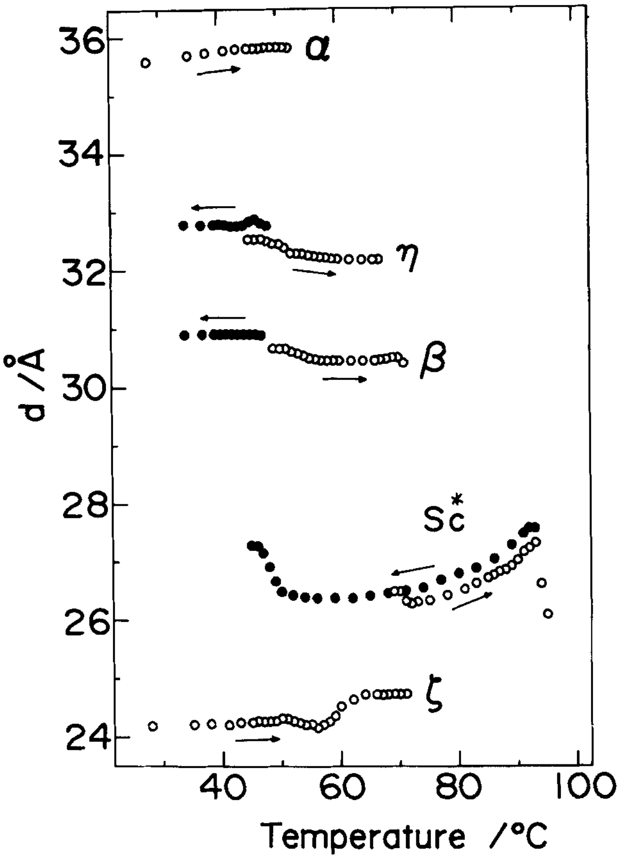

FIGURE 6 Temperature dependence of the X-ray lattice spacings estimated from the data of Figure 4.

the δ and ε forms, especially, a band at 415 cm^{-1} is prominent, which is characteristic of the twisted conformation of the biphenyl group as clarified for a wholly-aromatic ester compound.[14,15] As shown below, this band is detected commonly in the liquid crystalline phase of compounds having the biphenyl group in the skeletal chain. The δ and ε forms are obtained by rapid cooling or quenching from the isotropic phase. The observation of the intense 415 cm^{-1} Raman band suggests an existence of the twisted biphenyl structure in the δ and ε forms, which is considered to result from the freezing of the thermally agitated twist motion of the biphenyl rings.

Phase Transitions as Revealed by the X-Ray and FTIR/Raman Measurements

As an example, the transitions starting from the α crystal form will be described in detail. The DSC thermogram measured on the α form is illustrated in Figure 3. In a temperature region of 50–60°C, a broad endothermic peak is observed and the α form transforms finally into the β form. However, the transition is not so simple and other types of solid phase take part in this transition. In Figure 4 is

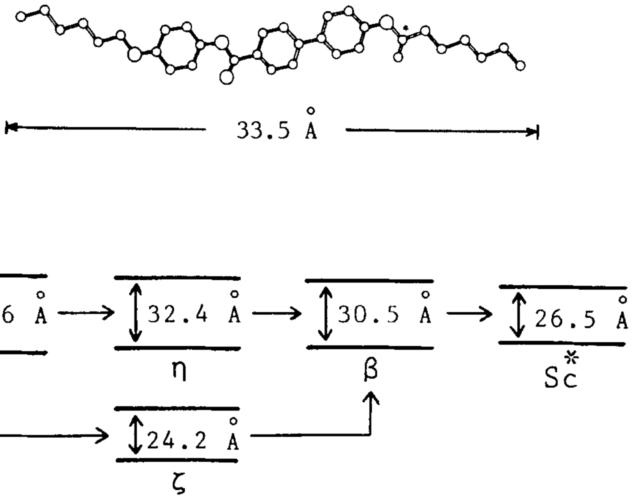

FIGURE 7 An illustration of the change in the interlayer spacing in the transition processes from the α to the S_c^* phase. The molecular model at the top is the fully extended structure.

shown the temperature dependence of the X-ray diffraction powder pattern. Figure 5 shows the temperature dependences of the peak intensities in the heating process. The two reflections at $2\theta = 2.5°$ and 3.6° detected at room temperature originate from the two independent crystal forms of α and ζ. As the temperature rises, the X-ray intensity of the α form decreases and that of the ζ form begins to increase around 42°C. At about 46°C the peak of another form, η, begins to appear and increases in intensity. This peak continues to grow even after the intensity of the ζ form is saturated at about 52°C. As the temperature rises further, the ζ peak decreases in intensity and the β form grows steeply. The η peak begins to decrease in intensity at about 58°C, where the relative intensity of the β form increases further. The β form generated in this way transforms into the smectic C phase (S_c^*) at about 71°C. These X-ray data allow us to extract the two types of the phase transitional route from the α to the β forms, as illustrated below.

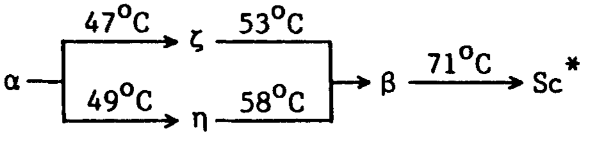

The transition temperatures between two phases were roughly estimated from the inflection points of the intensity vs. temperature curves in Figure 5 (indicated by vertical rods). The ζ or η form is often contained in the starting α form. Although the ζ and η forms look like to behave independently of each other as shown in Figures 4 and 5, it is unclear, at present, whether the transition occurs, even partially, between them in addition to the ζ → β and η → β transitions.

The temperature dependence of the lattice spacings estimated from the low-angle X-ray reflections is shown in Figure 6. Taking into account the chain length of a

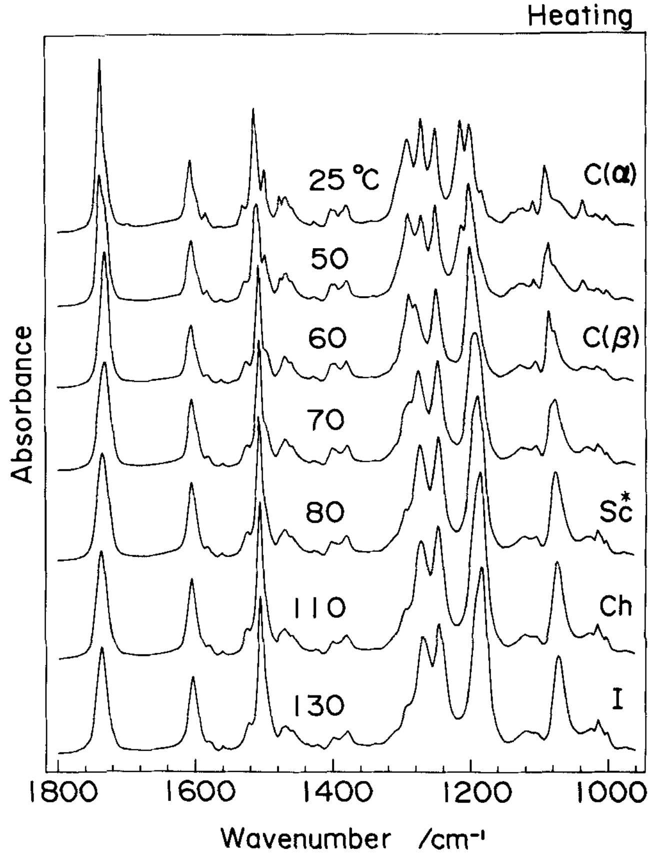

FIGURE 8 Temperature dependence of the infrared spectra, starting from the α form in the frequency region of 1000–1800 cm^{-1}.

fully extended molecular structure of about 34 Å, the spacings of these reflections are considered to correspond to the interlayer distances in the solid and liquid crystal phases. In the transition route of $\alpha \rightarrow \eta \rightarrow \beta \rightarrow S_c^*$, the interlayer distance exhibits a stepwise reduction, suggesting a stepwise increase of the tilt angle of the chain measured from the normal to the layer plane (Figure 7). In the route of $\alpha \rightarrow \zeta \rightarrow \beta \rightarrow S_c^*$, on the other hand, the change is rather anomalous: the *d*-spacing decreases once from 36 Å (α) to 24 Å (ζ) and increases again up to 30 Å (β). Although the exact index of the reflection at $d = 24.2$ Å is not determined yet, this value seems too large to be ascribed to a lateral spacing. As a possible explanation of such anomalous change in lamellar spacing, we consider an occurrence of lamellar structural change between a normal segregated lamella (α or β) and an interpenetrative-type one (ζ).

Structural Changes in the $S_c^* \rightleftharpoons$ Ch Ferroelectric Phase Transition

In Figure 6 is also shown the temperature dependence of the interlayer distance in the transition region of $S_c^* \rightarrow$ Ch. With a rise of temperature, the interlayer

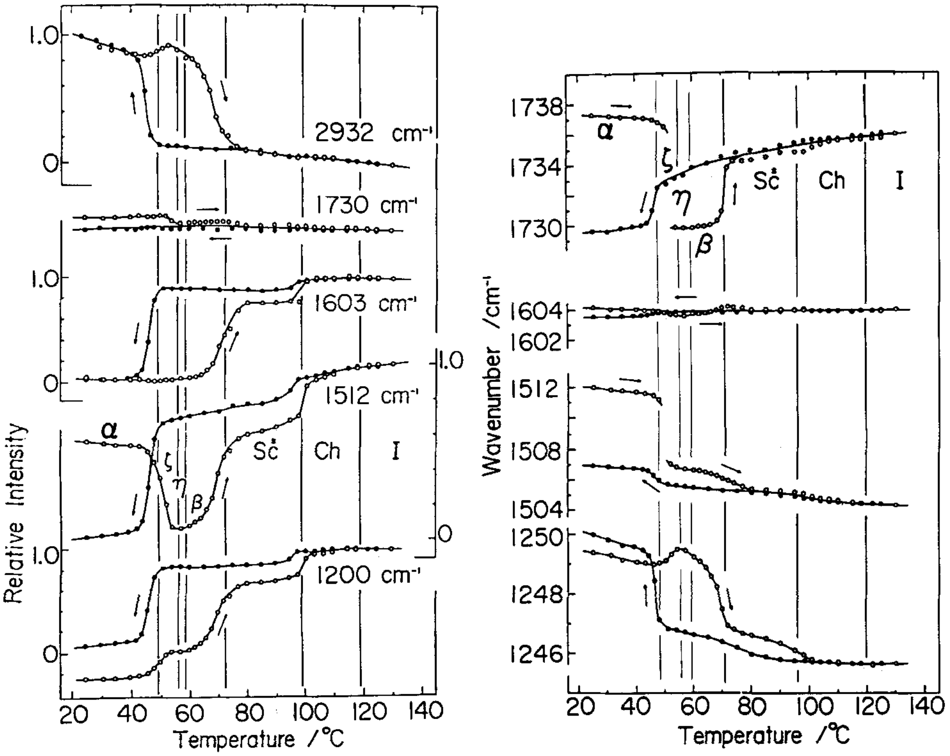

FIGURE 9 Temperature dependences of the relative intensity and wavenumber estimated for the various infrared bands.

distance increases gradually and attains a maximum at temperature a little below the Curie transition point (T_c). Such behavior of the interlayer spacing gives a direct and microscopically-viewed evidence for a change in the molecular layer thickness and corresponds well to the change in the macroscopically observed helical pitch.[11-13] In many papers, the temperature dependence of the helical pitch is related qualitatively to that of the tilt angle of the *rigid* chain. But, such a simple relation cannot be applied in the present system. That is to say, the actual molecule is not so rigid in the liquid-crystalline phase, but the flexibility of the molecular chain must not be overlooked. In Figure 8 is shown the temperature dependence of the infrared spectra in the frequency region of 1000–1800 cm^{-1}. The temperature dependences of the relative intensity and peak frequency of the several infrared bands are shown in Figure 9. At each stage of the phase transitions from the α to β through the ζ or η phase, the relative intensity and/or peak position of the bands changes drastically. The flexible alkyl part of the molecule is highly disordered in the liquid-crystalline phases as seen in the large decrease in the associated band intensity (at 2932, 1460 cm^{-1}, etc.). The bands relating to the benzene or ester groups (at 1730, 1603, 1512 cm^{-1}, etc.) change their intensity and peak position not only in the $\alpha \rightarrow \beta$ but also in the $S_c^* \rightarrow$ Ch transition, indicating that the mesogen groups experience further conformational change even in the $S_c^* \rightarrow$ Ch

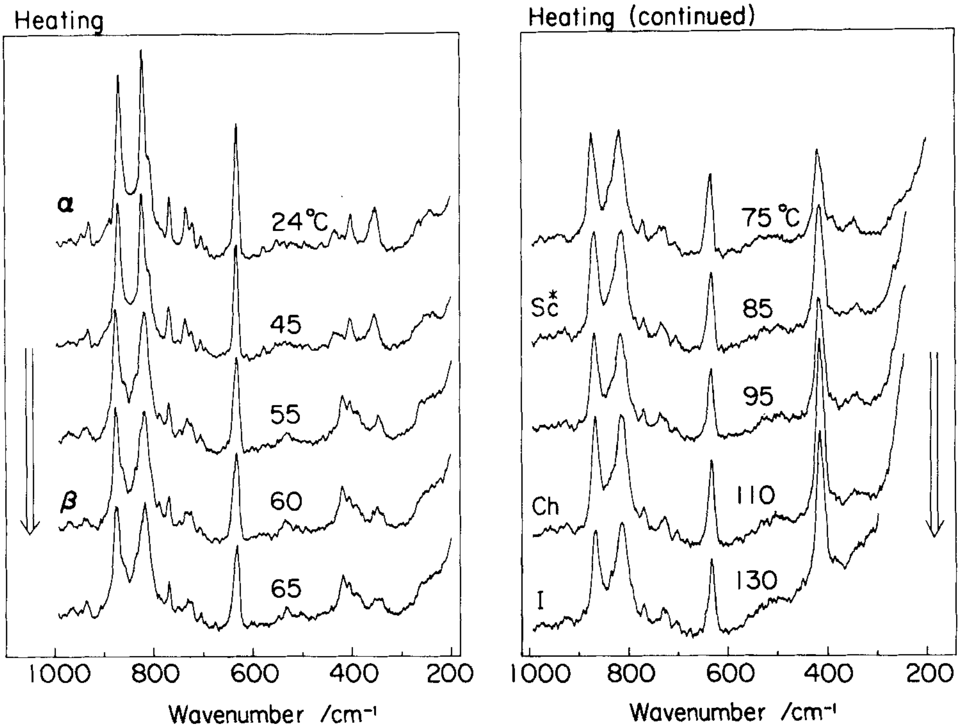

FIGURE 10 Temperature dependence of the Raman spectra, starting from the α form.

transition. In Figure 10 is reproduced the temperature dependence of the Raman spectra measured, starting from the α form. The spectra change largely in the vicinity of the transition stages from the α to the β forms via the ζ and η forms. Based on the X-ray diffraction data described above, the Raman spectra at 45°C may consist of both the α and ζ (and η) forms and those at 55°C may consist of the β and η forms. Roughly speaking, the spectra of the ζ form are not so different from those of the α form and the spectra of the η form are also not so different from those of the β form, although the decrease in intensity may indicate some disordering in the ζ, η and β forms. The band at 415 cm^{-1} increases in intensity remarkably when the β form transforms into the S_c^* phase. This band further increases in intensity at the $S_c^* \rightarrow$ Ch phase transition. As reported already,[14,15] this band associates with the "twisted" biphenyl conformation. It should be noticed here that the relative intensity of this band increases gradually but steadily on the way from the β to the S_c^* phases. That is to say, the biphenyl group changes the conformation gradually in the temperature region of the ferroelectric phase transition. The polarity of the molecule is mainly due to the

part. Therefore, the dipole moment of the whole molecule is sensitive to the dihedral angle of the

bond. Although it is not known at present whether the twisting of the biphenyl group is static or dynamic, such a conformational change could become a direct trigger for the temperature change in the bulk spontaneous polarization in the S_c^* phase.

Acknowledgment

This work was partly supported by a Grant-in-Aid for Scientific Research on Priority Areas, New Functionality Materials—Design, Preparation and Control, by the Ministry of Education, Science and Culture, Japan.

References

1. R. B. Meyer, L. Liebert, L. Strzelecki and P. Keller, *J. Phys. (Paris) Lett.*, **36**, L-69 (1975).
2. R. B. Meyer, *Mol. Cryst. Liq. Cryst.*, **40**, 33 (1977).
3. Ph. Martinot-Lagarde, *J. Phys. (Paris)*, **38**, L-17 (1977).
4. K. Yoshino, T. Uemoto and Y. Inuishi, *Jpn. J. Appl. Phys.*, **16**, 571 (1977).
5. J. Hoffmann, W. Kuczynski and J. Malecki, *Mol. Cryst. Liq. Cryst.*, **44**, 287 (1978).
6. N. A. Clark and S. T. Lagerwall, *Appl. Phys. Lett.*, **36**, 899 (1980).
7. K. Miyasato, S. Abe, H. Takezoe, A. Fukuda and E. Kuze, *Jpn. J. Appl. Phys.*, Suppl. **22**, 661 (1983).
8. K. Yoshino, M. Ozaki, T. Sakurai, K. Sakamoto and M. Honma, *Jpn. J. Appl. Phys.*, Suppl. **23**, 175 (1984).
9. S. Garoff and R. B. Meyer, *Phys. Rev. Lett.*, **38**, 848 (1977).
10. Ph. Martinot-Lagarde, R. Duke and G. Durand, *Mol. Cryst. Liq. Cryst.*, **75**, 249 (1981).
11. H. Takezoe, K. Kondo, A. Fukuda and E. Kuze, *Jpn. J. Appl. Phys.*, Suppl. **21**, 627 (1982).
12. K. Kondo, H. Takezoe, A. Fukuda and E. Kuze, *Jpn. J. Appl. Phys.*, Suppl. **21**, 224 (1982).
13. K. Kondo, S. Era, M. Isogai and A. Mukoh, *Jpn. J. Appl. Phys.*, Suppl. **24**, 1389 (1985).
14. K. Tashiro, J. Hou, M. Kobayashi and T. Inoue, *J. Am. Chem. Soc.*, **112**, 8273 (1990).
15. K. Tashiro, J. Hou and M. Kobayashi, *Rep. Progr. Polym. Phys. Jpn.*, **32**, 415 (1989).